

# Dynamic Performance of a 30-kW Microturbine-Based CHP System

A. Y. Petrov

A. Zaltash

S. D. Labinov

D. T. Rizy

R. L. Linkous

Cooling, Heating, and Power (CHP) Group  
Engineering Science and Technology Division  
Oak Ridge National Laboratory (ORNL)

## ABSTRACT

*The goal of the Cooling, Heating, and Power (CHP) Program established in 2000 by the US Department of Energy (DOE) is to provide research, development, testing (both laboratory and field) and to accelerate implementation of distributed electric generation (DG) with thermally-activated technologies (TAT). The objective is to provide DG with waste heat recovery, i.e. combination of DG and waste heat recovery utilization to drive various TAT units (heat recovery, desiccant, absorption chiller units, etc.) and increase overall fuel efficiency of the technology. Dynamic tests of the CHP system, which were performed at the CHP Integration Laboratory of the Oak Ridge National Laboratory (ORNL), are presented. The CHP system at the Lab includes: a 30-kW microturbine generator, an air-to-water heat recovery unit, an indirect-fired single-effect 10-ton (35-kW) absorption chiller, and indirect- and direct-fired desiccant dehumidification units. The dynamic system response of the CHP system was tested during both cold-startup and power-dispatch (changing electric/thermal demand) modes. The test results provide valuable information for both understanding CHP performance as well as for use to develop better control tools for CHP equipment.*

## INTRODUCTION

DOE's Cooling, Heating, and Power (CHP) Program was established in 2000. Its primary purpose is to provide research, development and testing in order to accelerate implementation of distributed electric generation (DG) with thermally-activated technologies (TAT). The objective of the CHP Integration Laboratory is to provide a test bed for testing combined electric power generation and waste heat recovery utilization to drive various TAT units (NEP 2001). The benefits of CHP include having both electric and thermal energy available from the same system and increasing overall fuel efficiency. CHP system performance is an important aspect since some of these systems are intended to be used during backup/emergency situations, and the time needed to reach a certain electrical/thermal demand from a cold start or during a load change becomes a crucial limiting factor. Also, the results of dynamic testing provide valuable data needed to create a dynamic model of the CHP system, and provide input for developing better control hardware and software for the technology. The dynamic performance of the 30-kW microturbine generator, which is a component of the CHP system presented in this paper, was previously outlined by Langley et al. (2002), Rizy et al. (2002), and SCE (2004). Dynamic performance aspects of the CHP system with direct-fired desiccant dehumidification unit are given by Petrov et al. (2004), so it is not considered in this paper.

## NOMENCLATURE

AC	- absorption chiller
AHU	- air handling unit
CHP	- combined cooling, heating, and power
COP	- coefficient of performance
DFDD	- direct-fired dehumidification unit
HHV	- higher-heating value of natural gas
IFDD	- indirect-fired dehumidification unit
HRU	- heat recovery unit
MTG	- microturbine generator

$Q_{\text{chilled}}$	- cooling capacity of absorption chiller
$Q_{\text{HRU}}$	- heat recovered by the HRU
$T_{\text{amb}}$	- ambient temperature
$T_{\text{HRU hot water out}}$	- hot water outlet temperature of the HRU
$T_{\text{AC chilled water out}}$	- chilled water outlet temperature of the AC
$W_{\text{MTG}}$	- electric power output of the MTG

## SYSTEM CONFIGURATION AND TEST EQUIPMENT

The CHP system, which was tested at the CHP Integration Laboratory, consists of a 30-kW microturbine generator (MTG), an air-to-water heat recovery unit (HRU), an indirect-fired (hot water-fired) 10-ton (35 kW) single-effect absorption chiller (AC) with air handling unit (AHU), an indirect-fired desiccant dehumidification unit (IFDD), and a direct-fired desiccant dehumidification unit (DFDD) (Zaltash 2003). The CHP system diagram is shown in Figure 1. The IFDD was used in these tests as a variable thermal load on the HRU's output (water side). There is an insulated air-duct ventilation system from the MTG's exhaust to the HRU and to the DFDD. The flow from either of these TAT units is controlled via dampers. Also, there is a water loop from the HRU to the IFDD and/or AC. Finally, there is an air mixing chamber leading to the air-duct system of the DFDD (for mixing outside air with exhaust air to lower its temperature and/or supplement its volume). The HRU, which is designed to capture the waste heat from the MTG exhaust gas, is used to produce hot water for the AC or IFDD or both. The insulated duct system and the air mixing with outside air are used to provide the hot air required for the DFDD. It is important to note that all of the individual equipment for the CHP system used in this study is commercially available, so the test results produced can indeed be interpreted as if it were a field installation. The instrumentation used at the CHP Integration Laboratory along with their measurement precisions is given in Table 1.

**TABLE 1**  
**Instrumentation and Measurement Precisions at the CHP Integration Laboratory**

Measurement	Sensor	Range	Precision
Temperature	Resistive temperature detector	-328 to 1,562 °F (-200 to 850 °C)	±0.2 °F (±0.1 °C)
Dew-point temperature	Chilled mirror	-40 to 140 °F (-40 to 60 °C)	±0.2 °F (±0.1 °C)
Dew-point temperature	Humidity/temperature transmitter	-40 to 140 °F (-40 to 212 °C)	±0.4 °F (±0.2 °C)
Air flow	Fan evaluator*	500 to 5,000 scfm (14.2 to 141.6 m <sup>3</sup> /min)	±2%
Water flow	Flow meter	0 to 100 gpm (0 to 0.38 m <sup>3</sup> /min)	±1%
Gas flow - DFDD	Pulse count test meter 10 pulses/cf	0 to 200 cfh (0 to 5.7 m <sup>3</sup> /h)	±0.2%
Gas flow - MTG	Pulse count test meter 10 pulses/cf	0 to 415 cfh (0 to 11.8 m <sup>3</sup> /h)	±0.2%
Gas pressure – DFDD	Pressure transducer	0 to 15 in wc (0 to 3.73 kPa)	±0.5% of full scale
Gas pressure – MTG	Pressure transducer	0 to 200 in wc (0 to 49.73 kPa)	±0.5% of full scale
Power – MTG	Watt transducer	0 to 40 kW (0 to 136,577 Btu/h)	±0.5% of full scale

\*A multi-point, self-averaging Pitot traverse station with integral air straightener-equalizer honeycomb cell, capable of continuously measuring fan discharges or ducted airflow.

## CASE STUDIES

The aim of this study was not to generalize the behavior of all possible combinations of CHP systems which would be beyond the scope of this study. This work was initiated to show the dynamic behavior of two specific CHP system combinations. The first case tested an MTG, HRU, and IFDD configured CHP system (the latter used as the

heating load) during cold-start and ramping of electric/thermal load (i.e. transition from one load to another). The second case tested a MTG, HRU, AC and AHU (the latter used as the cooling load) configured CHP system.

### Case Study No. 1: MTG+HRU+IFDD CHP System

**Cold-Startup:** The “cold-startup” tests of the MTG+HRU+IFDD CHP system configuration were performed at two different MTG electric power output levels – 20 (20 net) and 30 (28 net) kW. Except for the different electric outputs, the remaining parameters influencing the CHP system performance (ambient temperature, HRU water flow rate and thermal load) were nearly the same for both tests. The HRU thermal load was controlled by maintaining constant process and regeneration air flow rates to the IFDD, as well as the dry-bulb air inlet temperatures. The test results are presented in Table 2 and Figures 2-5. Table 2 presents the different lengths of time (transient time) required to reach steady-state operating conditions for key MTG and HRU parameters. Steady-state conditions were reached when percent deviation (ratio of standard deviation to running or moving average value over a certain range) of each parameter was equal or less than the specified value in Table 2. Figures 2-5 provide detailed insight into the most important thermal performance parameters, such as heat recovered by the HRU, the HRU hot water inlet/outlet temperatures, and the MTG/HRU exhaust gas temperatures.

Note that the cold-start of this CHP system configuration is to some extent a step-wise process: for example the heat recovery process does not begin simultaneously with the MTG startup. The HRU operates in a “bypass” mode which isolates the heat exchanger from the MTG exhaust gas by the HRU's diverter valve until the temperature of MTG exhaust gas at the inlet to HRU reaches a temperature set-point value ( $195 \pm 5^\circ\text{F}$ , or  $90.5 \pm 2.5^\circ\text{C}$ ). The HRU uses the bypass mode to avoid condensation of the MTG's flue gas in the HRU. Upon reaching the required set-point temperature, the HRU diverter switches from the bypass to the “recovery” mode. The spike in the data of Figure 5, which shows the dynamics of the HRU outlet gas, is related to the bypass/recovery process. Prior to the spike the bypass mode is "on" so the temperature increases until it reaches  $\sim 195^\circ\text{F}$  ( $90.5^\circ\text{C}$ ) at which time the recovery mode turns "on". The lead time in these tests before the start of heat recovery was  $\sim 4$  minutes which impacted the remaining thermal parameters. Therefore, two transient times are shown in Table 2 and Figures 2-5 to differentiate between the start of the MTG and the start of heat recovery. The first transient time, which is shown without parenthesis, relates to the MTG startup. The second transient time, which is shown in parenthesis, relates to the start of heat recovery.

**TABLE 2**  
**Transient Times of MTG+HRU+IFDD CHP System to Reach Steady-State after Cold Startup**

	CHP system startup with MTG set for 20 kW			CHP system startup with MTG set for 30 kW		
MTG power output, kW	20 (20 net)			30 (28 net)		
IFDD dry-bulb temperature, °F (°C)	95.0 (35.0)			95.0 (35.0)		
Ambient temperature, °F (°C)	35.0 (1.7)			41.0 (5.0)		
Parameter	Steady-state value	Percent deviation	Transient time, min	Steady-state value	Percent deviation	Transient time, min
MTG power output, kW	20.0	<0.5	4	28.0	<0.5	4
MTG exhaust gas outlet temperature (after recuperator), °F (°C)	470.6 (243.7)	<0.2	20	523.7 (273.2)	<0.2	23
HRU exhaust gas outlet temperature, °F (°C)	180.3 (82.4)	<0.2	68 (64)	212.6 (100.3)	<0.2	75 (71)
Heat recovered by HRU, Btu/h (kW)	111,137.2 (32.6)	<2.0	34 (30)	152,990.3 (44.8)	<2.0	55 (51)
HRU hot water inlet temperature, °F (°C)	152.3 (66.8)	<0.2	56 (52)	182.1 (83.4)	<0.2	59 (55)
HRU hot water outlet temperature, °F (°C)	163.1 (72.8)	<0.2	56 (52)	197.3 (91.8)	<0.2	59 (55)

The testing parameters of Table 2 and Figures 2-5 indicate that the MTG reaches steady-state performance much faster than the HRU indicating that the HRU and water load to the HRU have a higher thermal inertia. For example, for the CHP system with the MTG set to 30 (28 net) kW, the MTG reaches a steady-state electric output in

4 minutes after startup, but the heat recovered by the HRU doesn't reach steady-state until 55 min after startup. Subsequently, the HRU hot water temperatures and the HRU exhaust gas temperature don't reach steady-state until 59 and 75 min after the MTG startup, respectively. As is evident from the comparison of the CHP system at the two power settings, the lower power setting at 20 kW results in a decrease in the transient times for both MTG and HRU performance. As compared to the 30 (28 net) kW setting, the MTG and heat recovered by HRU for the CHP system with the MTG setting of 20 kW are nearly proportional to the ratio of the settings (i.e., 20/28 or 0.71).

Based on the test data the time constants of the major performance parameters were calculated. The time constant indicates the interval needed for the parameter to reach 63% of its new value in response to a step input change (Palm 1986). The results are given in Table 3.

The time constant results also show that, apart from the heat recovered parameter, the HRU part of the CHP system has much more inertia than the MTG part. The largest time constant of the CHP system is attributed to the exhaust gas temperature leaving the HRU. In addition, time constants seem to be somewhat independent of the electric and associated thermal energy.

**TABLE 3**  
**Time Constants of Key MTG+HRU+IFDD CHP System Parameters**

Parameter	Electric power output, kW	Initial value	New (steady-state) value	Percent deviation	63% of new value*	Time constant, min
MTG electric power output, kW	20 (20 net)	0	20	<0.5	12.6	3.5
	30 (28 net)	0	28	<0.5	17.6	3.5
Heat recovered by HRU, Btu/h (kW)	20 (20 net)	0	111,137.2 (32.6)	<2.0	70,076.4 (20.5)	3.0
	30 (28 net)	0	152,990.3 (44.8)	<2.0	96,383.9 (28.2)	3.0
MTG exhaust gas out temperature, °F (°C)	20 (20 net)	70.3 (21.3)	470.6 (243.7)	<0.2	322.5 (161.4)	3.5
	30 (28 net)	51.4 (10.8)	523.7 (273.2)	<0.2	348.9 (176.1)	4.0
HRU exhaust gas out temperature, °F (°C)	20 (20 net)	105.0 (40.6)	180.3 (82.4)	<0.2	152.4 (66.9)	17.0
	30 (28 net)	105.0 (40.6)	212.6 (100.3)	<0.2	172.7 (78.2)	16.0
HRU hot water in temperature, °F (°C)	20 (20 net)	85.0 (29.4)	152.3 (66.8)	<0.2	127.4 (53.0)	15.0
	30 (28 net)	85.0 (29.4)	182.1 (83.4)	<0.2	146.2 (63.4)	15.0
HRU hot water out temperature, °F (°C)	20 (20 net)	85.0 (29.4)	163.1 (72.8)	<0.2	134.2 (56.8)	14.5
	30 (28 net)	85.0 (29.4)	197.3 (91.8)	<0.2	155.8 (68.8)	14.5

\*Hereinafter defined as (new value – initial value) · 0.63 + initial value

**Ramping of Electric/Thermal Load:** The ramping tests were performed to study the dynamic performance of the same CHP system (MTG+HRU+IFDD) for changes in electric/thermal outputs and to measure the system response time. The case study covers different electric/thermal power modes (Table 4). The electric power output was controlled by changing the MTG electric power output setting. The heat recovered by the HRU (the thermal demand) was controlled by changing the dry-bulb temperature of the IFDD. Figures 6 and 7 present the results obtained during this study.

**TABLE 4**  
**Ramping of Electric and Thermal Load for the MTG+HRU+IFDD CHP System**

Condition No.	Elapsed time period, min	Electric load, kW	Thermal load, kBtu/h (kW)	Figure No.
1	0-60	30 (28 net)	155 (45.4)	6
2	61-120	30 (28 net)	165 (48.3)	6
3	121-244	30 (28 net)	155 (45.4)	6
4	245-314	20 (20 net)	118 (34.6)	7
5	315-260	20 (20 net)	127 (37.2)	7
6	361-430	20 (20 net)	118 (34.6)	7

For Figure 6 the MTG power output is held constant at 30 (28 net) kW while for Figure 7 it is constant at 20 kW. Note that the change in the thermal demand was achieved by changing the dry-bulb temperature of the IFDD

from 80 to 50°F (26.7 to 10.0°C); the higher dry-bulb temperature corresponded to the production of higher temperature hot water and lower heat recovered by the HRU (thermal demand).

Figures 6 and 7 show the variation of the basic parameters in the course of the test, namely: electric power output; heat recovered by the HRU (thermal demand); inlet and outlet hot water temperatures of the HRU; dry-bulb temperature of the IFDD, and ambient temperature. The latter, as well as the HRU water flow rate (not shown), were almost constant during the test (36-38°F or 2.2-3.3°C and 20.5 gpm or 77.6 L/min, respectively).

The tests show that the transition time for step change in electric power output is less than one minute (i.e., 20 seconds), but the time needed for stabilization of the hot water temperature is within 37-48 minutes, although heat recovered by the HRU reaches steady-state much faster (after 5-24 minutes). Therefore, the hot water temperature is the CHP performance parameter with the longer time constant. It should be noted that the time values given are only valid for certain electric outputs, thermal loads and ambient temperatures. The tests didn't consider MTG power settings of less than 20 kW. However, it may be possible to model the entire range of CHP dynamic performance using a number of reference points for different values of the above mentioned parameters to describe the transition processes with relatively simple mathematical functions such as algebraic equations. Such a model could provide a means for operators to optimize the performance of their CHP system, i.e., efficiency, heat output, electrical output, time to increase power, etc. Also, such a model could provide a means to develop better software and hardware to control electrical and thermal conditions for the CHP equipment.

### Case Study No. 2 – MTG+HRU+AC CHP System

The “cold-startup” of the MTG+HRU+AC CHP system was performed from zero to the maximum available MTG electric power output of 22.9 kW (what was possible at the ambient temperature of 82°F or 27.8°C). The CHP system was operated with the AC water flow rates close to nominal values, hot water flow of 38.0 gpm (143.8 L/min), chilled water flow of 28.0 gpm (106.0 L/min), and cooling water flow of 64.3 gpm (243.4 L/min).

The results of the test, which was run over a 3-hour period, are shown in Figures 8 and 9. Figure 8 shows the dynamic behavior of the major thermal parameters, such as AC cooling capacity and chilled water outlet temperature, heat recovered by the HRU and the HRU hot water outlet temperature. Figure 9 shows the dynamics of the MTG and the total CHP efficiencies, as well as the coefficient of performance (COP) of the AC unit.

The dynamic pattern of some of the CHP parameters (for example, HRU hot water temperature or  $Q_{HRU}$ ) during cold startup is slightly different from the previous CHP system configuration. The reason is that, apart from the IFDD not being part of the system and thus not providing a smooth change in thermal load, the AC starts to produce cooling capacity only upon reaching and maintaining a set-point hot water temperature (usually around 160°F, or 71°C). Prior to the temperature of the HRU outlet hot water reaching this temperature, the AC operates in a “bypass” mode. Thus, there is no thermal load for the HRU with the AC in bypass mode so the hot water temperature increases very rapidly. As soon as the AC switches from “bypass” to “recovery” mode, it starts to produce chilled water ( $Q_{chilled}$ ), and the hot water temperature continues to rise, but slowly until it reaches steady-state. The bypass/recovery modes of the AC explain the initial large slope of the heat recovery ( $Q_{HRU}$ ) and hot water outlet temperature curves of Figure 8.

As seen in Figure 8, the time between the MTG startup (at “0” elapsed time) and the start of AC operation ( $Q_{chilled} > 0$ ) could reach 20 minutes. Unfortunately, the operational conditions of the HRU component of the CHP system can't always provide successful start of the AC operation with the first attempt. The first attempt doesn't always produce sufficient thermal input to the AC unit (set-point hot water temperature required to operate the AC could not be maintained). It was found that it usually requires two to three attempts before the AC starts to produce useful cooling capacity. The fluctuations caused by these attempts are not shown in Figure 8 in order to simplify it. In addition, the time constants do not include these attempts. The time between HRU and AC startups is usually 10-15 minutes. The use of hotter MTG exhaust or a more effective HRU could significantly reduce the AC startup time or ensure successful startup with the first attempt. Tests with the current CHP configuration determined that the transition time to reach steady-state for the AC (cooling capacity and chilled water temperature) is ~70 minutes from the MTG startup or 50 minutes from the AC successful startup.

Figure 9 shows the dynamic trends of the HHV-based MTG and total CHP efficiencies, as well as the COP of the AC, which are calculated according to Zaltash et al. (2003). Results show that the transient times are tied to the MTG startup and similar to those of the AC cooling capacity and the chilled water outlet temperature, i.e. dynamics of total CHP efficiency is governed by the AC performance. The time constants of the major performance parameters for this CHP system are shown in Table 5. Note that the values for the AC are much lower than for the HRU.

Figure 10 shows the effect of ambient temperature on the dynamic behavior of the MTG from cold start to maximum available power output at full (30 kW) power setting. Results show an increase in transient time with

ambient temperatures. This seems to be the result of the controller and control scheme used by the manufacturer of this MTG.

**TABLE 5**  
**Time Constants of Key MTG, HRU and AC Parameters**

Parameter	Initial value	New (steady-state) value	Percent deviation	63% of new value	Time constant, min
MTG electric power output, kW	0	22.9	<1.2	14.3	4.5
AC cooling capacity, Btu/h (kW)	0	107,392.5 (31.5)	<3.0	67,657.3 (19.8)	3.0
AC chilled water out temperature, °F (°C)	81.1 (27.2)	47.0 (8.3)	<0.9	59.6 (15.3)	1.5
Heat recovered by HRU, Btu/h (kW)	0	166,477.4 (48.8)	<2.0	104,880.8 (30.7)	7.5
HRU hot water in temperature, °F (°C)	80.8 (27.1)	172.6 (78.1)	<0.5	138.6 (59.2)	8.0
HRU hot water out temperature, °F (°C)	80.8 (27.1)	181.6 (83.1)	<0.5	144.3 (62.4)	9.0

## CONCLUSIONS

A series of CHP system tests were performed with different combinations of commercially available equipment to measure the transition times and time constants for reaching steady-state operation during cold startup and after load ramping. The test results show that the thermally-activated components of the CHP systems have much more thermal inertia than the MTG (electric generator) component. The dynamic performance of the MTG component of the CHP system for the most part varies nearly proportionally to the net power output of the MTG. The largest time constant of the CHP system is attributed to the HRU exhaust gas temperature. The activation modes of the HRU and AC directly impact the transition times of the CHP system. They both operate with bypass/recovery modes which activate only when the input temperature reaches a set-point value. In the case of the HRU, the set-point of the inlet temperature of the HRU or the MTG exhaust gas temperature must be ~195°F (90.5°C) before the HRU switches from the bypass to the recovery mode. In the case of the AC, the set-point of the inlet temperature of the AC or the HRU water outlet temperature must reach ~160°F (71°C). These type of test results provide important insight to CHP performance characteristics and valuable input for model development that can be used in simulation of dynamic performance and implementation of better control tools for CHP systems. Future testing of a CHP system with a larger MTG is planned to evaluate how the increased size and make may affect dynamic time constants. It is important to note that the time constants measured during these tests are also a function of the existing controls and control schemes used by the various CHP system components (i.e., the MTG). It should be noted that this study only addresses the dynamic behavior of two specific commercially available CHP combinations. Furthermore, the electric generator is of only one type (MTG) and further CHP system testing using different generators (i.e., reciprocating engines) is planned to gather information on their dynamic performance characteristics.

## ACKNOWLEDGEMENTS

The authors would like to thank the Office of Energy Efficiency and Renewable Energy, U.S. Department of Energy (DOE), for supporting this work. This research was also supported in part by an appointment to the Oak Ridge National Laboratory (ORNL) Postdoctoral Research Associates Program administered jointly by the Oak Ridge Institute for Science and Education and ORNL. This work was conducted by ORNL under DOE contract DE-AC05-00OR22725 with UT-Battelle, LLC.

## REFERENCES

- Langley, R., T. Key and D.T. Rizy. 2002. Steady-state and dynamic performance characterization testing of a microturbine. Proceedings of the Power System Conference "Impact of Distributed Generation", March 13-15, 2002, Clemson, SC, pp. 1-6
- NEP. 2001. Reliable, affordable, and environmentally sound energy for America's future. Report of the National Energy Policy Development Group. Washington, DC: U.S. Government Printing Office.
- Palm, V.J. 1986. Control system engineering. New York, NY: John Wiley & Sons, Inc.
- Petrov, A.Y., A. Zaltash, E.A. Vineyard, S.D. Labinov, D.T. Rizy, and R.L. Linkous. 2003. Baseline and IES performance of a direct-fired desiccant dehumidification unit under various environmental conditions. Proceedings of the 2003 Annual ASHRAE Meeting, June 27-July 02, 2003, Kansas City, MO, paper KC-03-5-2.
- Petrov, A.Y., A. Zaltash, E.A. Vineyard, S.D. Labinov, D.T. Rizy, and R.L. Linkous. 2004. Baseline, exhaust-fired, and combined operation of desiccant dehumidification unit. Paper submitted to the 2004 ASME International Mechanical Engineering Congress and Exposition, November 13-19, 2004, Anaheim, CA, paper IMECE2004-60264.
- Rizy, D.T., A. Zaltash, S.D. Labinov, A.Y. Petrov, and P.D. Fairchild. 2002. Integration of distributed energy resources and thermally-activated technologies. Proceedings of the Power System Conference "Impact of Distributed Generation", March 13-15, 2002, Clemson, SC, pp. 1-6.
- SCE. 2004. Behavior of Capstone and Honeywell microturbine generators during load changes, Public interest energy research final report, publication 500-04-033, prepared For California Energy Commission. Rancho Cucamonga, CA: Southern California Edison.
- Zaltash, A., A.Y. Petrov., D.T. Rizy, S.D. Labinov, E.A. Vineyard, and R.L. Linkous. 2003. Laboratory research on integrated energy systems (IES). Proceedings of the 21<sup>st</sup> International Congress of Refrigeration, August 17-22, 2003, Washington, DC, paper ICR0203.

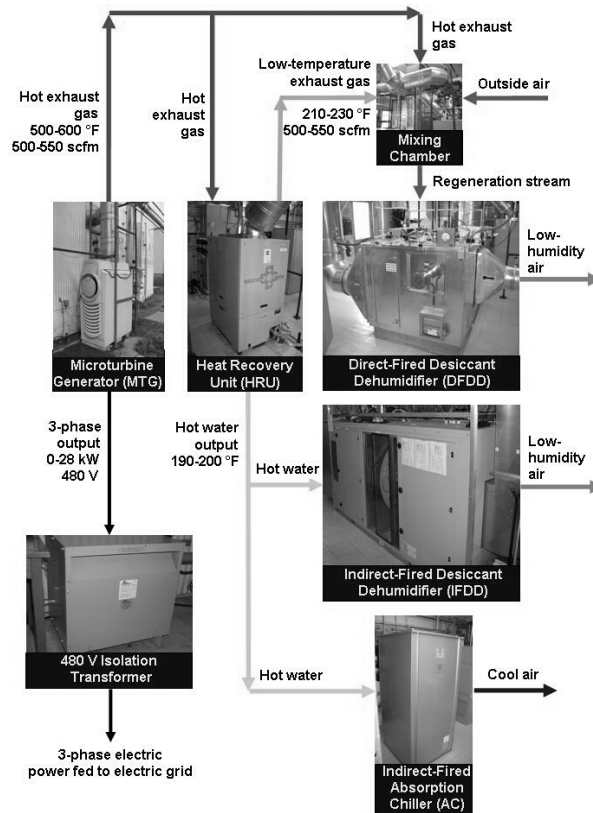
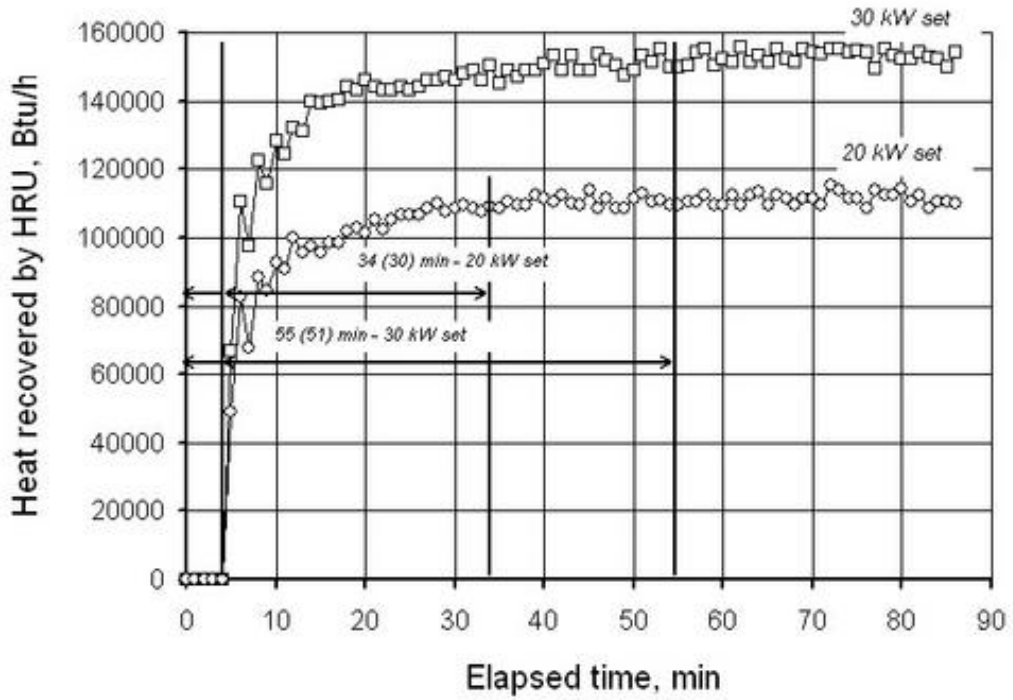
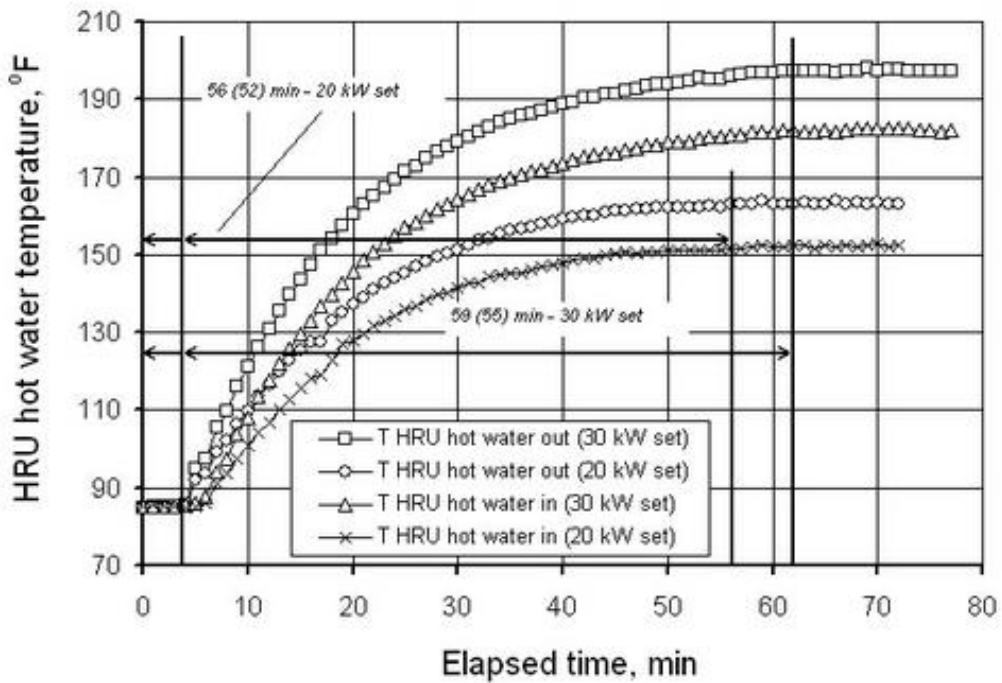


Figure 1 CHP Integration Laboratory showing components presently under study



**Figure 2** Dynamic performance of heat recovered by HRU of the MTG+HRU+IFDD CHP system during cold startup with two MTG electric power output settings



**Figure 3** Dynamic performance of HRU hot water temperature of the MTG+HRU+IFDD CHP system during cold startup with two MTG electric power output settings

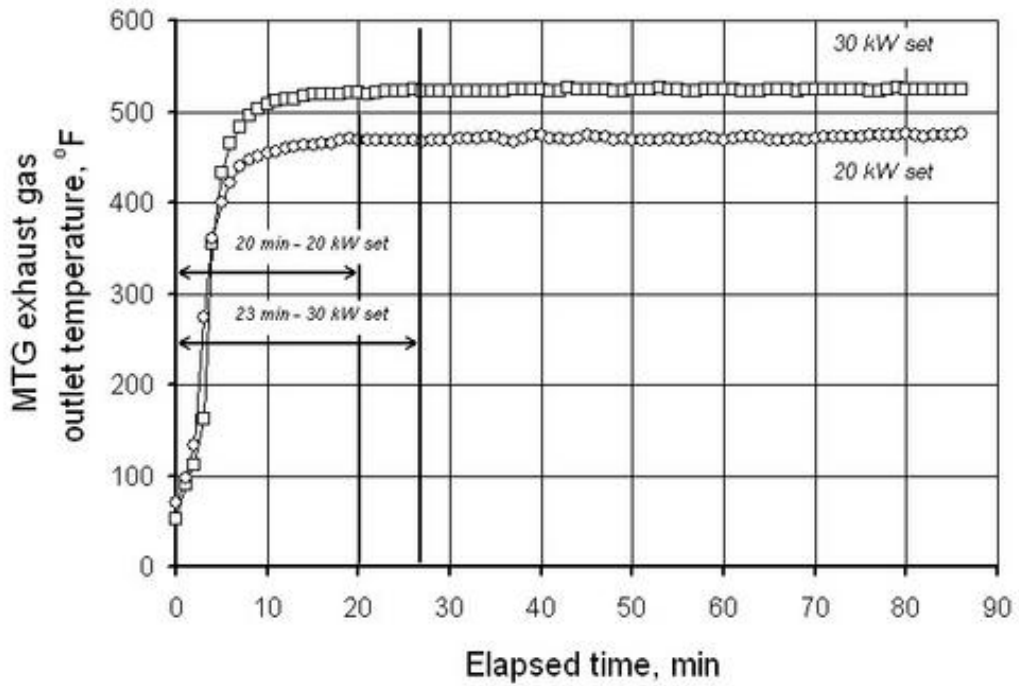


*Figure 4* Dynamic performance of MTG exhaust gas outlet temperature of the MTG+HRU+IFDD CHP system during cold startup with two MTG electric power output settings

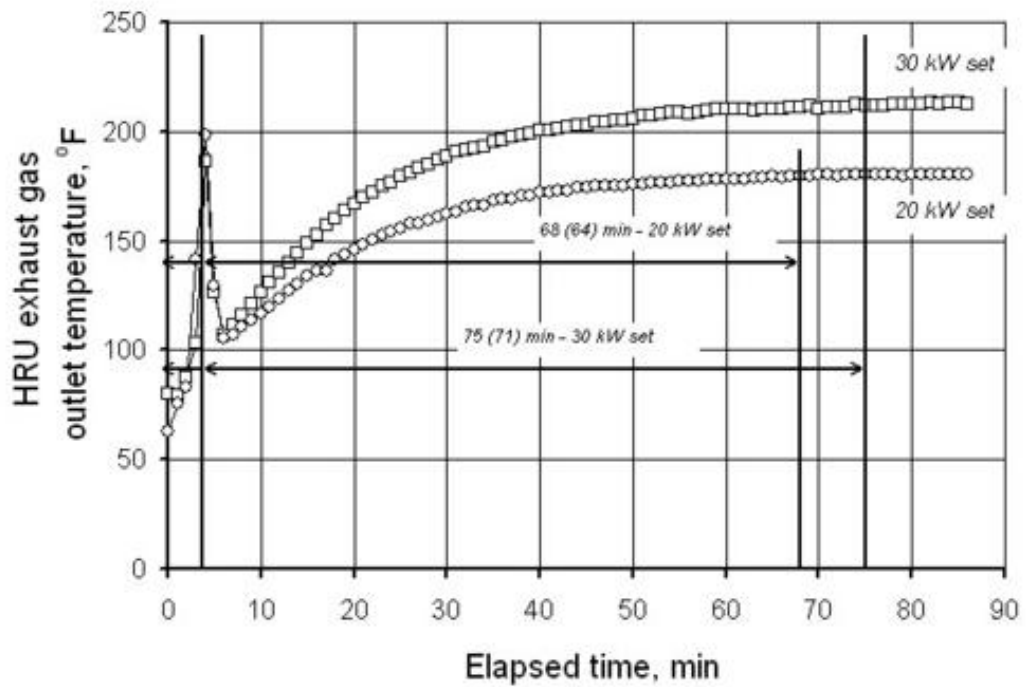


*Figure 5* Dynamic performance of HRU exhaust gas outlet temperature of the MTG+HRU+IFDD CHP system during cold startup with two MTG electric power output settings

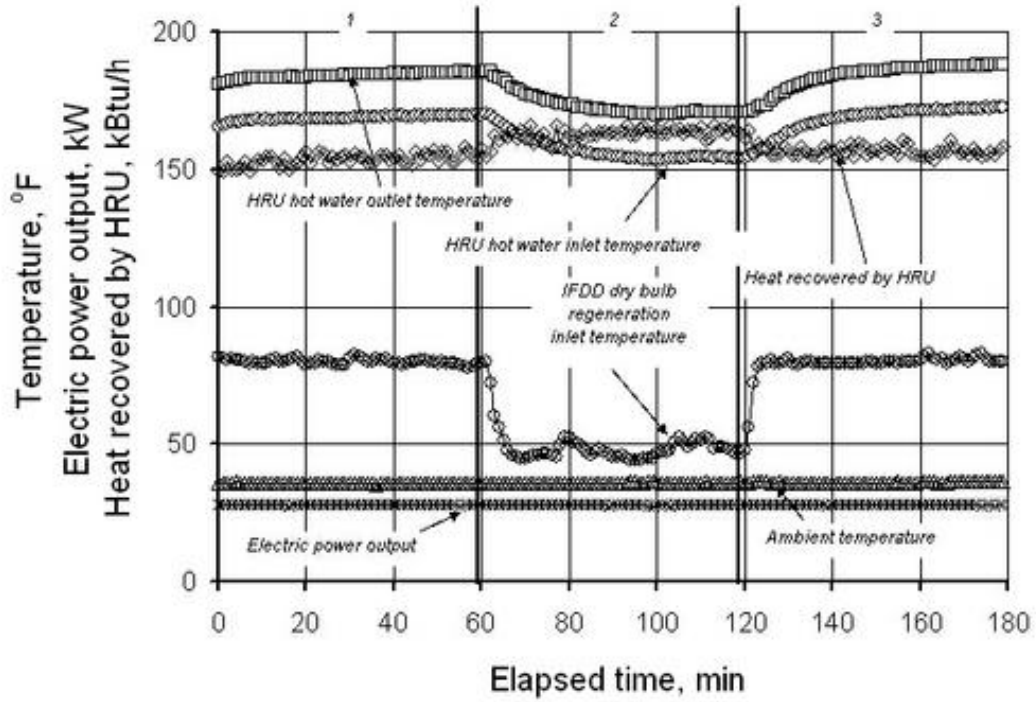


Figure 6 Dynamic performance of the MTG+HRU+IFDD CHP system with thermal load ramping  
 $W_{MTG} = 30$  (28 net) kW

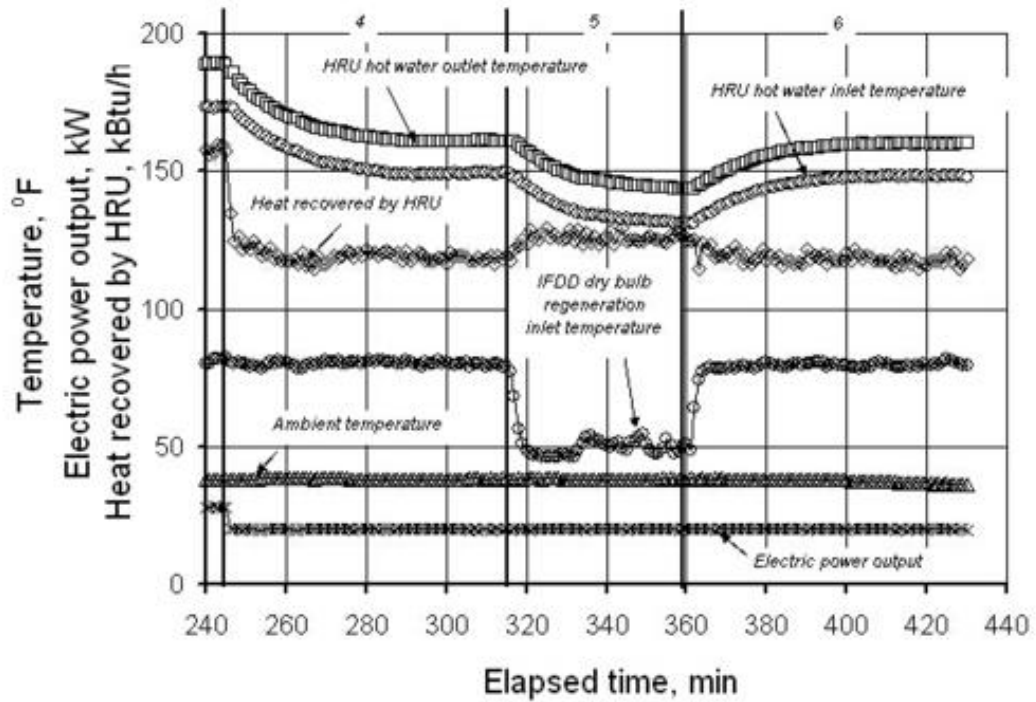


Figure 7 Dynamic performance of the MTG+HRU+IFDD CHP system with thermal load ramping  
 $W_{MTG} = 20$  (20 net) kW

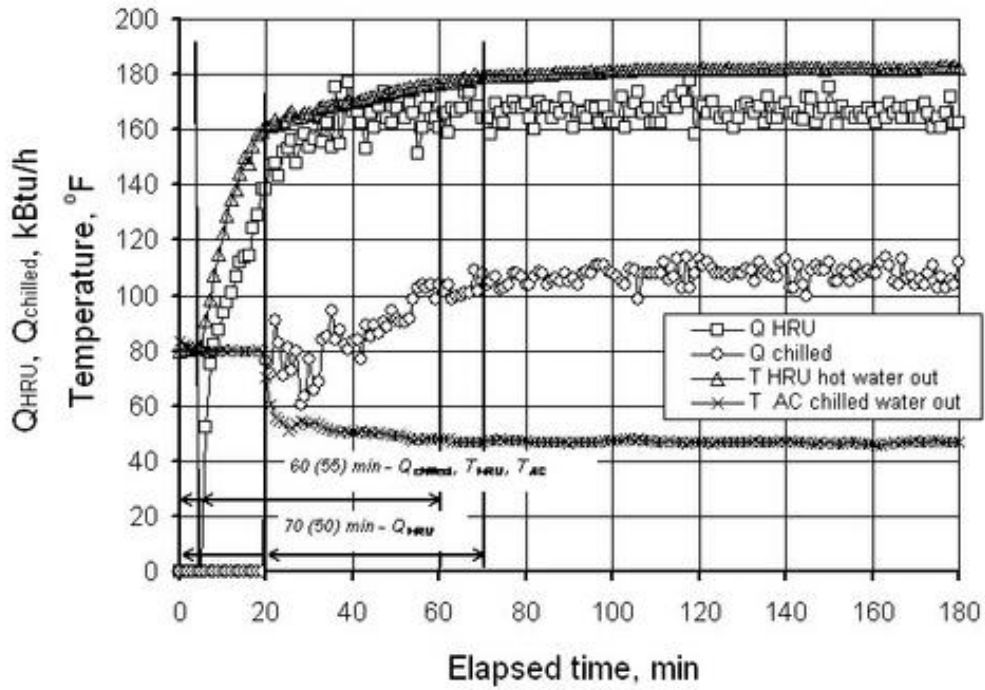


Figure 8 Dynamic performance of thermal parameters of the MTG+HRU+AC CHP system during cold startup

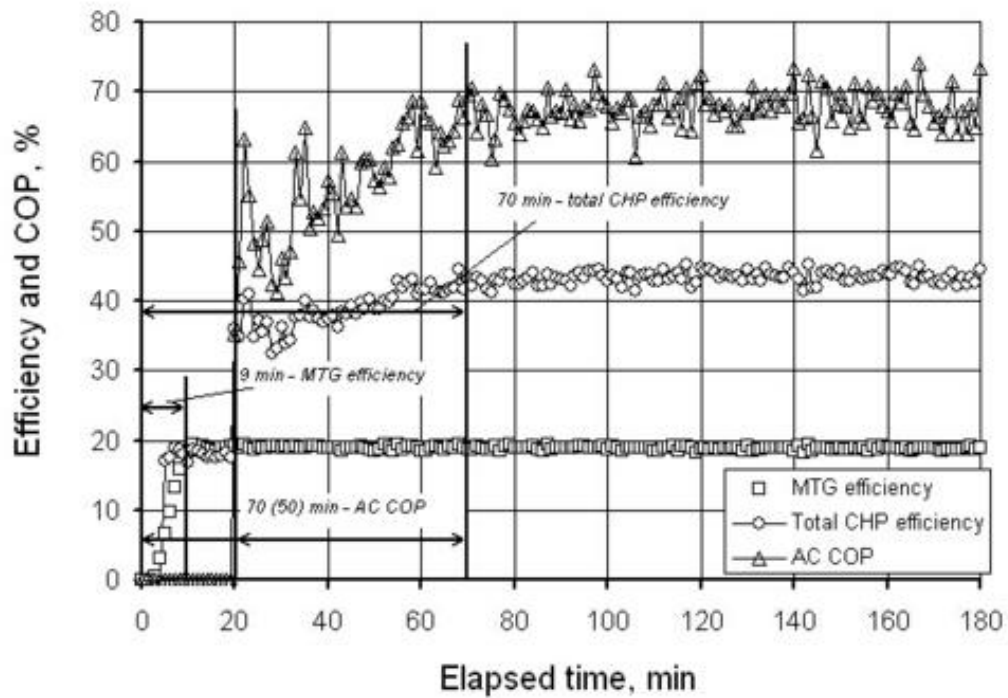
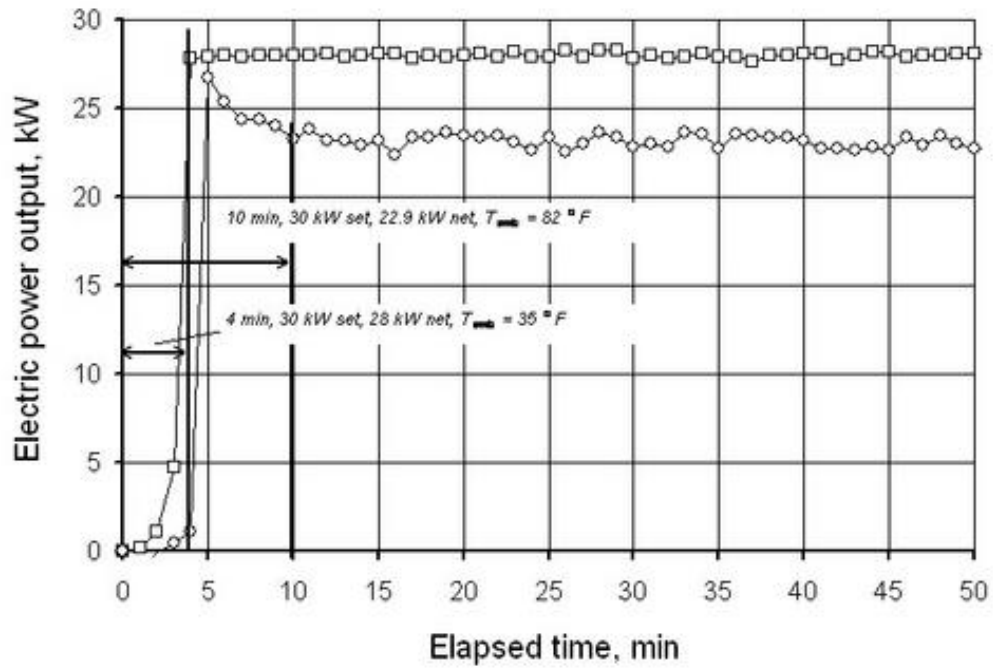


Figure 9 Dynamic performance of HHV-based MTG and total CHP efficiencies, and AC COP of the MTG+HRU+AC CHP system during cold startup



**Figure 10** Dynamic performance of net MTG electric power output during cold startup with different ambient temperatures